Iran. J. Ichthyol. (2026) 13(3): 168-186
P-ISSN: 2383-1561; E-ISSN: 2383-0964
© 2026 Iranian Society of Ichthyology

ORIGINAL ARTICLE

Projecting habitat suitability changes of *Caranx ignobilis* (Forsskål, 1775) in the Persian Gulf using ensemble species distribution models

Hamed MOUSAVI-SABET*, Abouzar HABIBI

Department of Fisheries, Faculty of Natural Resources, University of Guilan, Sowmeh Sara, Iran.

Correspondence
mousavi-sabet@guilan.ac.ir

Article history:
Accepted 15 September 2026

Abstract
Understanding the impacts of climate change on marine habitats is essential for predicting future species distribution patterns and supporting sustainable fisheries management, particularly for commercially important apex predators. In this study, we used occurrence records from global databases (GBIF and OBIS) and published field surveys, combined with Bio-ORACLE environmental predictors, to model current and future habitat suitability of *Caranx ignobilis* (Forsskål, 1775) in the Persian Gulf. We implemented six individual modeling algorithms and three ensemble modeling techniques using the biomod2 platform. The ensemble model EMwmean (AUC= 0.992, TSS= 0.923) was selected for final projections because it integrates multiple algorithms and reduces model-specific bias. Based on variable importance analysis, sea surface temperature (SST), salinity, and primary production were identified as the most influential environmental predictors shaping habitat suitability. Future projections under SSP2-4.5 and SSP5-8.5 indicated progressive contraction of suitable habitat in the southeastern Persian Gulf, accompanied by a northwestward displacement of the habitat centroid. Specifically, the modelled area classified as suitable habitat is projected to decline from $48.49\times10^3 km^2$ under current conditions to zero by the 2090s under both SSP2-4.5 and SSP5-8.5, reflecting zero modelled suitable habitat under the applied threshold rather than biological extirpation. These findings provide spatially explicit information to support adaptive fisheries management and conservation planning, thereby enhancing the long-term resilience of this ecologically and commercially important reef-associated predator under future climate change in the Persian Gulf.

Keywords: Climate change, Ensemble modeling, Persian Gulf, Habitat suitability, Species distribution

INTRODUCTION

Anthropogenic greenhouse-gas emissions have driven unprecedented increases in global surface temperatures since the mid-20th century. As the largest reservoir of heat and carbon in the Earth system, the oceans have absorbed most of this excess energy, causing ocean heat content to rise rapidly since the 1970s (IPCC 2021). Consistent with this warming trend, 2015–2024 was the warmest decade on record, with recent years ranking among the hottest ever observed (World Meteorological Organization 2024; Copernicus Climate Change Service 2024; NOAA/NCEI 2024). Continued accumulation of heat and CO_2 in the ocean has altered key physical and biogeochemical properties of marine ecosystems, including temperature, dissolved oxygen, pH, and primary productivity. These environmental changes have profound ecological consequences, influencing the distribution, abundance, and persistence of marine organisms. Climate-driven changes in marine environments threaten marine organisms by degrading habitats, altering community structure, and spreading non-indigenous species (Boyce et al. 2022; Nisin et al. 2023; Schickele et al. 2020a). These changes may have long-lasting and, in some cases, irreversible impacts on marine biodiversity, fisheries-dependent economies, and the sustainable management of marine resources. However, for some species, climate change may also create newly suitable environmental conditions, facilitating range expansions into previously unsuitable areas (Pitman et al. 2021).

The Persian Gulf has warmed rapidly in recent decades, with satellite-derived and in situ observations showing a persistent increase in sea surface temperature (SST) and some of the highest summer SSTs recorded worldwide (Bordbar et al. 2023; Lachkar et al. 2025). The Gulf's shallow, semi-enclosed basin, limited exchange with the open ocean, and intense solar radiation make it particularly vulnerable to heat accumulation compared with larger

marine systems (Alawad et al. 2023; Lachkar et al. 2025). This warming has increased the frequency and intensity of marine heatwaves, exacerbating coral bleaching and ecosystem stress across the region (Lachkar et al. 2025). These characteristics make the Persian Gulf one of the most climate-sensitive marine ecosystems, with substantial implications for the distribution and persistence of marine species.

Against this background, understanding and predicting how marine species respond to climate change has become a fundamental challenge for sustainably managing and conserving marine resources in the Persian Gulf. *Caranx ignobilis*, a reef-associated apex predator of considerable ecological and commercial importance, is strongly influenced by environmental variables such as sea surface temperature, salinity, primary productivity, and other physicochemical characteristics of the marine environment (Froese & Pauly 2024). Consequently, climate-driven changes in these environmental conditions are expected to alter the distribution and availability of suitable habitats for this species, particularly in warm, shallow, and environmentally sensitive systems such as the Persian Gulf (Cheung et al. 2015).

Caranx ignobilis (giant trevally) is a widely distributed Indo-West Pacific marine fish, occurring from the Red Sea and East Africa to the Hawaiian Islands and central Pacific, with a range extending north to southern Korea and Japan and south to Australia, New Caledonia, Tonga, and Rapa. It is also reported from the Persian Gulf and Gulf of Oman. According to the IUCN Red List, *C. ignobilis* is classified as Least Concern (LC) (Eagderi et al. 2026).

Species Distribution Models (SDMs) are widely used to identify current suitable habitats and to project species responses to climate change, but individual algorithms often rely on different statistical assumptions and can yield divergent forecasts (Elith & Leathwick 2009; Robinson et al. 2017). Ensemble modelling, which integrates multiple statistical and machine-learning algorithms, mitigates model-specific bias, better quantifies uncertainty, and typically improves predictive performance and robustness (Araújo & New 2007; Thuiller et al. 2019). However, despite the ecological and commercial importance of *C. ignobilis*, relatively few studies have used ensemble SDMs to assess current and future habitat suitability under climate change, particularly in the Persian Gulf. Therefore, an ensemble SDM framework provides a more robust approach to projecting climate-driven changes in *C. ignobilis* habitat suitability under SSP2-4.5 and SSP5-8.5 climate scenarios, reducing model-specific uncertainty and improving the reliability of future habitat projections.

To address these knowledge gaps, we applied six individual species distribution models (SDMs) and three ensemble models to assess the current and future habitat suitability of *C. ignobilis* in the Persian Gulf. Habitat suitability was projected under two Shared Socioeconomic Pathways (SSP2-4.5 and SSP5-8.5) using environmental predictors from Bio-ORACLE. Specifically, this study aimed to (i) identify the most accurate SDM for predicting the distribution of *C. ignobilis*, (ii) quantify the key environmental drivers shaping its current habitat suitability, and (iii) project changes in habitat suitability under contrasting climate scenarios for the mid-century (2040-2050) and end-century (2090-2100). The findings provide spatially explicit information for climate-adaptive fisheries management and conservation planning for this ecologically and commercially important species in the Persian Gulf.

MATERIALS AND METHODS

Species occurrence data: Occurrence records for this species were obtained from the Global Biodiversity Information Facility (GBIF; https://www.gbif.org/occurrence/; accessed on 4 October 2025), the Ocean Biodiversity Information System (OBIS; https://obis.org/search/; accessed on 15 October 2025), and published geo-referenced field surveys. Data from the three sources were merged, then cleaned and quality-controlled in QGIS (version 3.12). Cleaning involved removing duplicate records, excluding terrestrial points or those with missing coordinates, and eliminating records with obvious coordinate errors. To

minimize spatial sampling bias, we applied spatial thinning using the spThin R package (version 0.2.0; Aiello-Lammens et al. 2015), retaining only one occurrence point within a 10km radius. After thinning, the final dataset comprised 8,029 presence records, which were exported in CSV format and stored as R objects to ensure full reproducibility of subsequent analyses (Chamberlain et al. 2017; Provoost & Bosch 2022). All cleaned occurrence data were stored with the World Geodetic System 1984 (WGS84) geographic coordinate system. After cropping the global dataset to the Persian Gulf study area and applying the depth mask (2-200m), 104 presence records remained within the study area. These 104 records are a subset of the global dataset used for calibration and do not constitute a separate calibration sample.

Environmental data sources: The spatial and temporal dynamics of *C. ignobilis* resources are substantially influenced by a range of oceanographic and environmental factors. Selecting appropriate environmental variables is crucial for accurately predicting habitat suitability (Zhang et al. 2000; Lee et al. 2018; Schickele et al. 2020b; Torrejon-Magallanes et al. 2021; Han et al. 2023). Relevant studies have shown that SST, current velocity, pH, primary production, salinity, and depth significantly influence the distribution and habitat use of large coral reef predators, including carangids (Sudekum et al. 1991; Meyer et al. 2007; Lédée et al. 2015; Papastamatiou et al. 2015).

We used environmental data from the Bio-ORACLE (version 3.0) database (https://www.bio-oracle.org/, accessed on 20 December 2025) and the Global Marine Environment Dataset (GMED; http://gmed.auckland.ac.nz) to predict the potential distribution of *C. ignobilis*. Present day variables (2010-2020) and future projections under two climate scenarios (SSP2 4.5 and SSP5 8.5) were obtained for two time periods: mid-century (2040–2050) and end-century (2090-2100) (Tyberghein et al. 2011; Assis et al. 2024). As a coastal pelagic species, *C. ignobilis* has an ecological depth range of 2-200 m, based on FishBase and FAO reports (Froese and Pauly, 2024; FAO 2018). All layers were extracted at a spatial resolution of 0.083° × 0.083° and projected to the WGS84 coordinate system. This resolution (~9 km) is consistent with previous Persian Gulf studies (Ahmadi et al. 2023; Poorbagher & Eagderi 2024) and is appropriate for regional-scale modeling; however, we acknowledge it may not fully resolve fine-scale coastal and reef gradients, which we note as a limitation. To reduce overfitting, we performed multicollinearity analysis using Pearson correlation coefficients (via the 'corrplot' R package; Wei & Simko 2021) as recommended for "biomod2" applications (Gregorich et al. 2021). Initially, seven variables were considered (sea surface temperature, salinity, current velocity, depth, primary production, pH, and dissolved oxygen). Dissolved oxygen showed a very strong negative correlation with SST ($|r| > 0.97$) and was therefore excluded (Brunner et al. 2024). We acknowledge that excluding dissolved oxygen may bias future projections because oxygen decline under warming is not solely controlled by temperature-dependent solubility; this is noted as a limitation, and future studies with high-resolution dissolved oxygen data are encouraged to include it. After filtering, six variables were retained: sea surface temperature, salinity, current velocity, depth, primary production, and pH. The study area was restricted to the Persian Gulf. To achieve this, all global raster layers were cropped to the Persian Gulf boundaries (longitude 48°-56.4°E, latitude 24°-30.5°N) using the crop function in the terra R package. Calibration was performed using the global environmental layers, while projections were restricted to the Persian Gulf. To detect novel environmental conditions, we used clamping masks in biomod2.

All raster layers were resampled to 0.083° using bilinear interpolation to reduce computational demand; preliminary tests showed that this coarsening did not qualitatively affect the predicted patterns (Assis et al. 2024). A depth mask (2 to 200m) was applied to all layers to exclude terrestrial cells and unsuitable depth ranges. For full reproducibility, all analyses were performed in R version 4.5.0, using the "biomod2" package version 4.2-6.2 (Thuiller et al.

2025). Validation using occurrence points showed that over 99% of points fell on valid (non-NA) cells, with the remaining NAs corresponding to land or areas outside the study region. For future projections, environmental layers were prepared for the 2040s (2040-2050) and 2090s (2090–2100) under SSP2 4.5 and SSP5 8.5 scenarios, similarly harmonized, masked to the depth range, and saved in .grd and .rds formats.

Habitat suitability modeling

Construction of single models: All SDMs in this study were implemented using "biomod2" (https://cran.r-project.org/web/packages/biomod2/index.html). The model algorithms we constructed utilized six singles-model algorithms from the Biomod2 package, including Flexible Discriminant Analysis (FDA), Generalized Additive Model (GAM), Gradient Boosting Machine (GBM), Generalized Linear Model (GLM), Maximum Entropy (MAXNET), and Multivariate Adaptive Regression Splines (MARS)**.** The six single-model algorithms were calibrated using presence records and pseudo-absence datasets generated with the random sampling procedure implemented in the BIOMOD_FormatingData function. (Barbet-Massin et al. 2012). Therefore, we used the random sampling method of the BIOMOD_FormatingData function to generate five independent pseudo-absence datasets (PA1–PA5)**,** each containing 10000 pesudo-absent records. Pseudo-absences were drawn from the global environmental background, consistent with the global calibration domain, to avoid mismatch between presence and absence domains. The bm_Modeling Options function was employed to fine-tune the parameters of all models, ensuring optimal performance and control of overfitting: for GBM we used 1000 trees with a learning rate of 0.01 and a bag fraction of 0.5; for FDA we used the "Mars" method with degree 1; for GAM we restricted the basis dimension (k=4) and applied shrinkage; for GLM we used a linear model without interactions; for MAXNET we set the regularization multiplier to 1.5; and for MARS we limited the degree to 1 and used a penalty of 3. Each single-model algorithm was set to run 7 repetitions for evaluation, with 80% of the data randomly selected as training sets and 20% as validation sets for model reliability testing (Shi et al. 2023a). In total, six individual modelling algorithms were constructed, each with 7 results, resulting in 246 models for simulating the current habitat distribution of *C. ignobilis*.

Construction of ensemble models: Ensemble Species Distribution Models combine multiple single SDMs into a unified prediction method (Araujo & New 2007). Ensemble models offer a notable advantage in amalgamating forecasts derived from multiple individual models, thereby attenuating inherent biases and variances while augmenting the overall model's capacity for generalization. Therefore, this method has been used to predict the habitats of multiple marine species (Chen et al. 2021; Chen et al. 2023). In this research, three ensemble algorithms—weighted mean (EMwmean), committee averaging (EMca), and the mean (EMmean)— were used to integrate the six single-model algorithms from the Biomod2 package. Single models with True Skill Statistics (TSS) values exceeding 0.7 were selected to form the definitive ensemble model, ensuring that only the most accurate models were included to optimize the overall predictive performance. Environmental response curves were generated using the bm_PlotResponseCurves function in the biomod2 package based on the ensemble mean of the six final models (GBM, FDA, GAM, GLM, MAXNET, and MARS). This enabled us to visualize and analyze the relationships between the six environmental variables (sea surface temperature, salinity, current velocity, depth, primary production, and pH) and the probability of *C. ignobilis* presence. These response curves were essential for understanding how each environmental variable affects the species' habitat suitability and for identifying the optimal habitat conditions under these variables. Five potential distribution areas of *C. ignobilis* were generated (current, SSP2-4.5 mid-century, SSP5-8.5 mid-century, SSP2-4.5 end-century, and SSP5-8.5 end-century), and the EMwmean ensemble, which integrates multiple algorithms and reduces model-

specific bias, was selected for final projections to the potential distribution area of *C. ignobilis* under current conditions and for two future time periods (mid-century 2040–2050 and end-century 2090-2100) under two climate scenarios (SSP2-4.5 and SSP5-8.5).

Evaluation of model's accuracy: Evaluating model performance is crucial for selecting robust species distribution models (Nisin et al. 2023). The area under the receiver operating characteristic curve (AUC) and the true skill statistic (TSS) are key evaluation metrics in SDMs, each providing complementary insights into model performance (Allouche et al. 2006; Lobo et al. 2007; Kaky et al. 2020;). The AUC value ranges from 0 to 1, with higher values indicating better discriminatory ability; values > 0.8 generally indicate good model performance, while values > 0.9 denote excellent performance (Yang et al. 2022). TSS combines sensitivity (true positive rate) and specificity (true negative rate) into a single threshold-dependent measure, providing a balanced assessment of predictive performance. TSS ranges from −1 to 1, with higher values indicating greater accuracy (Allouche et al. 2006; Xu et al. 2024). These metrics facilitate the evaluation of predictive accuracy and reliability, supporting informed decisions on model selection and threshold determination. To detect potential overfitting, we calculated the difference between calibration (training) and validation performance for each model. Small differences indicated good generalization capacity, whereas large differences (i.e., calibration substantially higher than validation) indicated overfitting (Thuiller et al. 2009). The mean differences and associated standard deviations were computed for each algorithm and metric (TSS and AUC).

Habitat changes of *Caranx ignobilis* under future climate scenarios: In biomod2, the Habitat Suitability Index (HSI) represents the probability of species occurrence. The ensemble model's HSI was generated by combining predictions from six single-SDM algorithms using three ensemble algorithms: weighted mean (EMwmean), committee averaging (EMca), and mean (EMmean) (Thuiller et al. 2025). The raw HSI values (originally ranging from 0 to 1000) were normalized to 0–1 using min-max scaling based on the current suitability distribution as a fixed reference, ensuring consistent comparison across scenarios. To restrict the analysis to the Persian Gulf, all global raster layers were cropped to the Gulf's boundaries (longitude 48°–56.4°E, latitude 24°–30.5°N) using the crop function in the terra R package. To evaluate habitat changes under future climate conditions, we projected the selected ensemble (EMwmean) onto environmental layers for two time periods – mid-century (2040-2050) and end-century (2090-2100) – under two Shared Socioeconomic Pathways: SSP2-4.5 and SSP5-8.5 (Assis et al. 2024). All projections were performed using the BIOMOD_EnsembleForecasting function with clamping masks to detect novel environmental conditions, and the output continuous suitability layers (GeoTIFF format) were saved at a spatial resolution of 0.083°. For quantitative analysis, we applied a binary classification based on a locally optimized TSS threshold (0.414) derived from the ensemble model evaluation. This threshold was obtained by maximizing the True Skill Statistic across cross-validation replicates, ensuring an optimal balance between sensitivity and specificity. This threshold is a statistical decision rule for comparison, not a biological criterion, and was fixed before future projections and applied uniformly across all scenarios and time periods. Accordingly, cells with suitability values ≥ 0.414 were classified as suitable habitat, and those below as unsuitable. We note that “zero suitable habitat” refers to the absence of cells exceeding this threshold, and does not imply biological extirpation. The area (km²) of suitable habitat was calculated for the current and each future scenario using the cellSize function in the R package terra. To quantify habitat changes, we computed the area lost (suitable in current but unsuitable in future), area gained (unsuitable in current but suitable in future), and net change between each future scenario and the current baseline. All maps and area tables were

Iran. J. Ichthyol. (2026) 13(3): 168-186

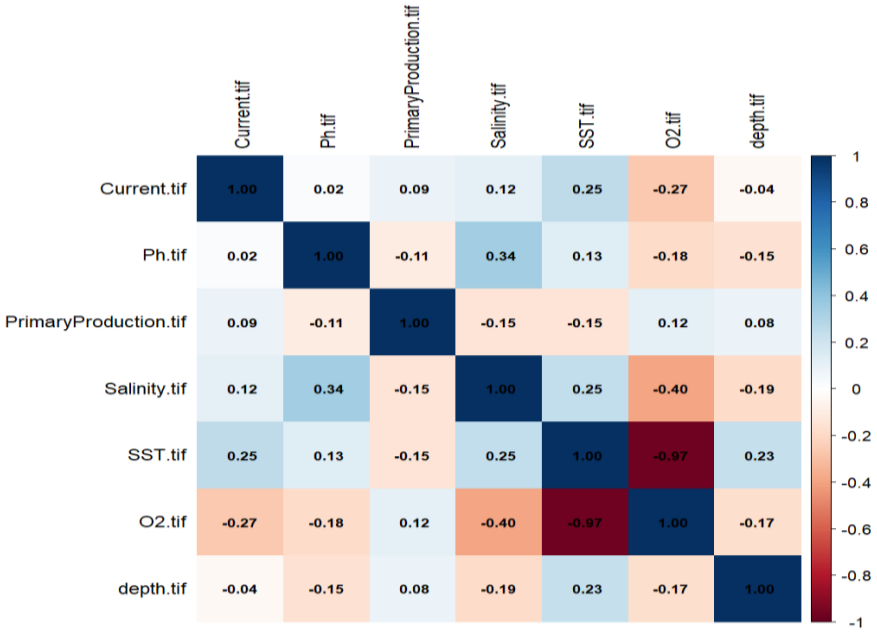


Fig.1. Heat map of Pearson correlation coefficients among the seven candidate environmental variables.

Table 1. Accuracy evaluation of single SDMs (SD1: represents the standard deviation of AUC; SD2: represents the standard deviation of TSS).

Evaluation	FDA	GAM	GBM	GLM	MARS	MAXNET
AUC	0.873	0.951	0.992	0.820	0.988	0.990
SD1	0.002	0.001	0.000	0.154	0.000	0.000
TSS	0.692	0.832	0.938	0.631	0.920	0.923
SD2	0.006	0.006	0.002	0.298	0.002	0.003

exported for visualization and subsequent statistical analysis.

Variation of latitude and longitude center of gravity of habitat: Habitat centroid shift is an important indicator for quantitatively assessing changes in species habitat distribution. By computing centroid shifts within suitable habitat for *C. ignobilis* under both present-day conditions and projected climate change scenarios, the response of *C. ignobilis* to climate-induced habitat shift can be evaluated. To define suitable habitat for centroid calculation, we applied a locally optimized TSS threshold (0.414) derived from the ensemble model evaluation, for the Persian Gulf region**,** meaning that only cells with HSI ≥ 0.414 were included in the centroid computation. The formulas for the longitudinal and latitudinal habitat centroids are as follows (Li et al. 2016):

(1) $\mathrm{LONG_{HSI}} = \sum_{i=1}^{K}(\mathrm{LONG}_i * \mathrm{HSI}_i)/\sum_{i=1}^{k} HSI_i$

(2) $\mathrm{LATG_{HSI}} = \sum_{i=1}^{K}(\mathrm{LATG}_i * HSI_i)/\sum_{i=1}^{k} HSI_i$

In the formulas, $\mathrm{LONG_{HSI}}$ and $\mathrm{LATG_{HSI}}$ represent the longitudinal and latitudinal centroid of HSI, respectively; i denotes the i-th cell, k is the total number of cells (excluding land and depths outside the species' vertical range), and HSI is the habitat suitability index (normalized 0-1) of the i-th site. All centroid calculations were performed in R using the terra package. To restrict the analysis to the Persian Gulf, all global raster layers were cropped to the Gulf's boundaries (longitude 48°-56.4°E, latitude 24°-30.5°N) using the crop function, and a land mask was applied to exclude terrestrial cells. A fixed min-max normalization was applied using the current suitability distribution within the Gulf as reference, ensuring consistent comparisons across scenarios. The shifts were quantified as the Euclidean distance (km) between the centroid of each future scenario and the current centroid. For scenarios where no suitable cells (HSI ≥ 0.414) were detected, centroid values were

Table 2. Accuracy evaluation of ensemble models.

Evaluation	EMca	EMmean	EMwmean
AUC	0.991	0.992	0.992
TSS	0.927	0.922	0.923

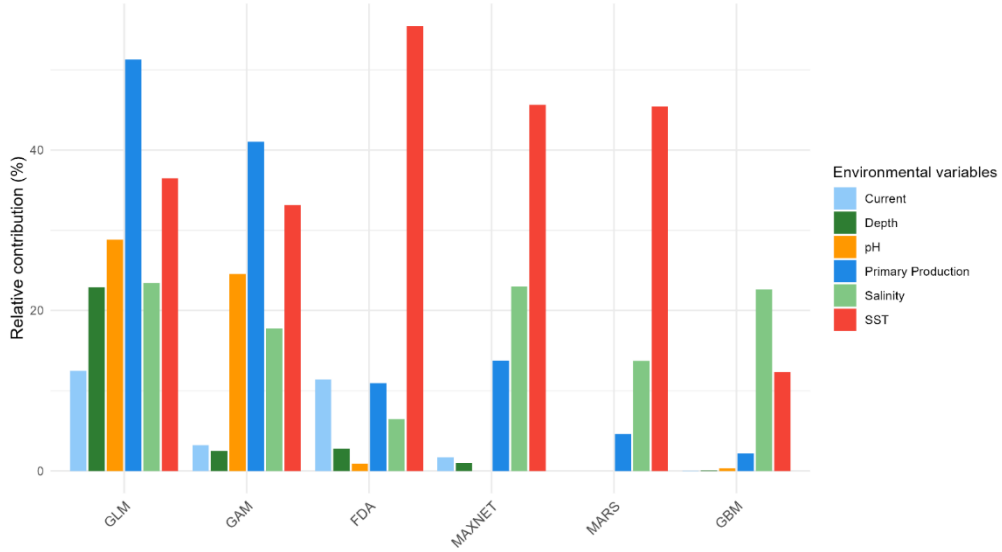


Fig.2. Average relative contribution rate of environmental factors of single SDMs.

recorded as NA, indicating zero modelled suitable habitat under the applied threshold rather than a complete biological loss.

RESULTS

Selection of environmental predictors: Selection of environmental predictors: Correlation analysis was conducted among the seven candidate environmental variables (Fig. 1). Dissolved oxygen showed a very strong negative correlation with sea surface temperature ($|r| > 0.97$) and was therefore excluded from further analyses to reduce multicollinearity. Among the remaining six environmental variables, most pairwise correlations were weak ($|r| < 0.4$), indicating no significant multicollinearity. These results suggest that the final predictor set showed low multicollinearity and was therefore suitable for species distribution modeling. The six retained variables—sea surface temperature (SST), salinity, current velocity, depth, primary production, and pH—were subsequently used to model the current and future habitat suitability of *C. ignobilis*.

Evaluation of model's performance

Performance evaluation of single models: Performance evaluation of single models: Based on the model results (Table 1), among the single SDMs, the GBM, MAXNET, and MARS models achieved the highest accuracy. Specifically, the GBM model achieved an AUC of 0.992 and a TSS of 0.938, while the MAXNET and MARS models had AUC values of 0.990 and 0.988 and TSS values of 0.923 and 0.920, respectively. The GAM model also showed good accuracy (AUC = 0.951, TSS = 0.832). In contrast, the FDA and GLM models showed relatively lower accuracy, with AUC values of 0.873 and 0.820 and TSS values of 0.692 and 0.631, respectively. All four models (GBM, MAXNET, MARS, and GAM) exceeded the predefined performance threshold (TSS > 0.7 and AUC > 0.9) and were therefore retained for ensemble modelling. The ensemble models were subsequently constructed using a TSS-based model selection criterion (TSS ≥ 0.7), retaining only model runs that satisfied this threshold.

Performance evaluation of ensemble models: Among the three ensemble models generated (Table 2), the weighted average (EMwmean) and committee averaging (EMca) algorithms showed similarly high accuracy. EMwmean achieved an AUC of 0.992 and

Iran. J. Ichthyol. (2026) 13(3): 168-186

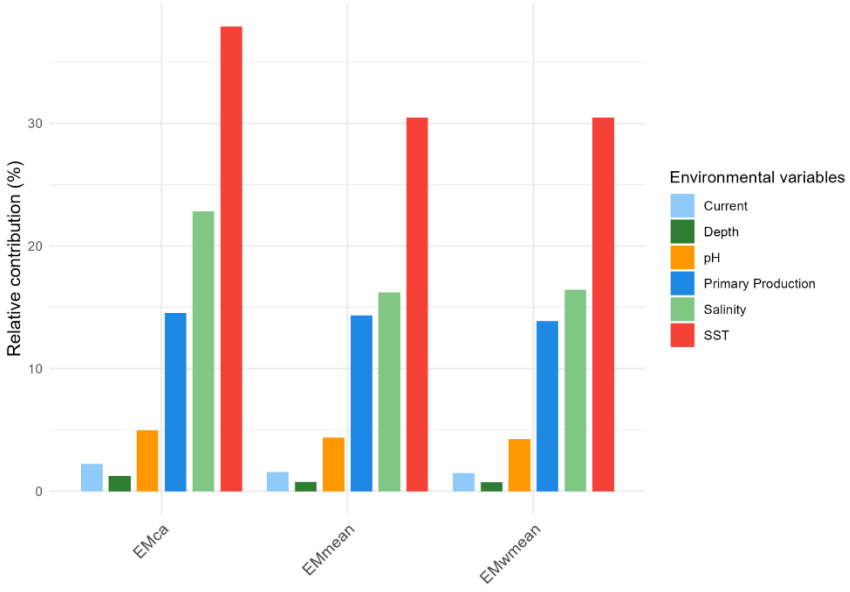


Fig.3. Average relative contribution rate of environmental factors of ensemble models.

a TSS of 0.923, while EMca showed an AUC of 0.991 and a TSS of 0.927. The mean ensemble (EMmean) performed slightly lower, though comparable, with an AUC of 0.992 and a TSS of 0.922. Given the nearly identical performance across all three ensemble algorithms, with marginal differences in TSS (≤ 0.005) and essentially equal AUC values, the three ensemble methods showed very similar predictive performance. EMwmean was selected as the final ensemble model because the weighted averaging approach assigns greater influence to better-performing single models. Therefore, EMwmean generated the final simulation results and projections.

Evaluation of the significance of environmental factors: Variable importance was first calculated for each of the six individual SDMs and subsequently summarized for the three ensemble models. The results (Fig. 2) indicate that, except for the GAM, GBM, and GLM models, SST exhibited the highest average relative contribution rate in the other three single models (FDA, MARS, and MAXNET), accounting for 63.1%, 71.2%, and 53.7%, respectively. In the GAM and GLM models, primary production had the highest average relative contribution rate (33.6% and 29.2%, respectively), followed by SST (27.1% and 20.8%, respectively). In the GBM model, salinity had the highest average relative contribution rate (60.3%), followed by SST (32.9%).

Among the three ensemble models constructed from the individual models that met the TSS > 0.7 criterion (Fig. 3), the average relative contribution rate of SST ranged from 45.3% to 45.6%, while that of salinity ranged from 24.4% to 27.3%, and that of primary production ranged from 17.4% to 21.4%. The cumulative contribution rate of these three factors exceeded 90%, indicating that SST, salinity, and primary production were the primary predictors influencing the distribution of *C. ignobilis* habitats. Furthermore, the average relative contribution rate of salinity exceeded 10% in most single models (except FDA) and in all ensemble models, highlighting its important contribution to habitat suitability. The environmental response curves (Fig. 4) showed distinct relationships between habitat suitability and the six environmental variables. Among the six predictors, primary production exhibited the highest suitability peak (0.412), followed by pH (0.175) and SST (0.165). The SST response curve peaked at approximately 26.3°C, beyond which suitability declined. Habitat suitability reached a local maximum at a salinity of approximately 35.2. For primary production, the highest suitability occurred at the lowest observed concentrations (optimal range 0.63–0.90mg/m³), indicating a declining relationship. In contrast, habitat suitability showed little sensitivity to

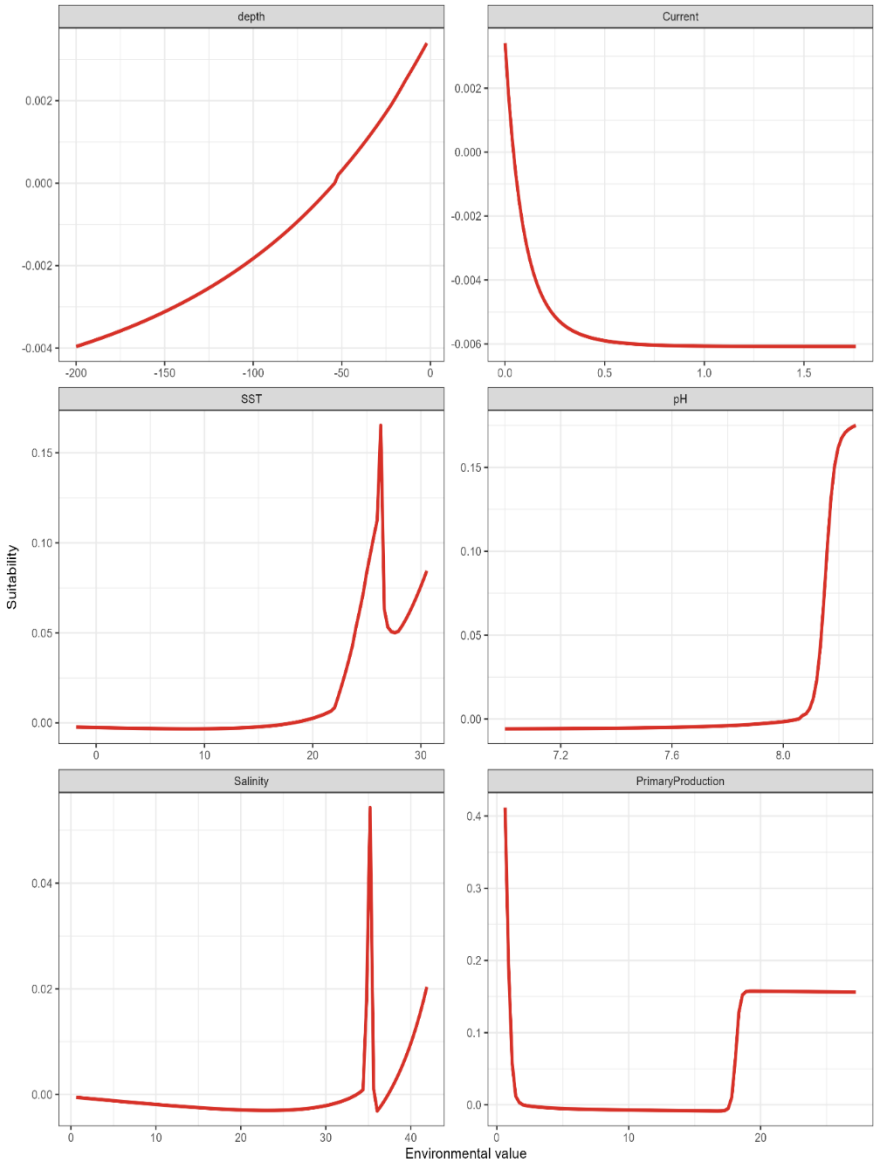


Fig.4. Response curves of the six environmental variables for *Caranx ignobilis* in the Persian Gulf. Curves represent the mean predicted habitat suitability across the six final models (GBM, FDA, GAM, GLM, MAXNET, and MARS). Each curve was generated by varying one environmental variable while holding the other variables at their median values. The y-axis represents habitat suitability (0–1), and the x-axis represents the environmental gradient.

current velocity across the observed gradient, with values remaining nearly constant at ~0.003. Habitat suitability increased slightly along the depth gradient, reaching its highest value (0.003) in shallow waters (2m). For pH, suitability increased toward higher values, peaking at approximately 8.26. Curves represent the mean predicted habitat suitability across the six final models (GBM, FDA, GAM, GLM, MAXNET, and MARS). Each curve was generated by varying one environmental variable while holding the other variables at their median values. The y-axis represents habitat suitability (0–1), and the x-axis represents the environmental gradient.

Distribution of current and future habitat changes of *Caranx ignobilis*: Based on the ensemble model output (Fig. 5), current habitat suitability of *C. ignobilis* within the Persian Gulf showed a distinct spatial gradient, decreasing from northwest to southeast. The highest suitability values (HSI approaching 1.0) were concentrated in the northwestern sector of the Gulf, between latitudes 28°N-30°N and longitudes 48°E–51°E, representing

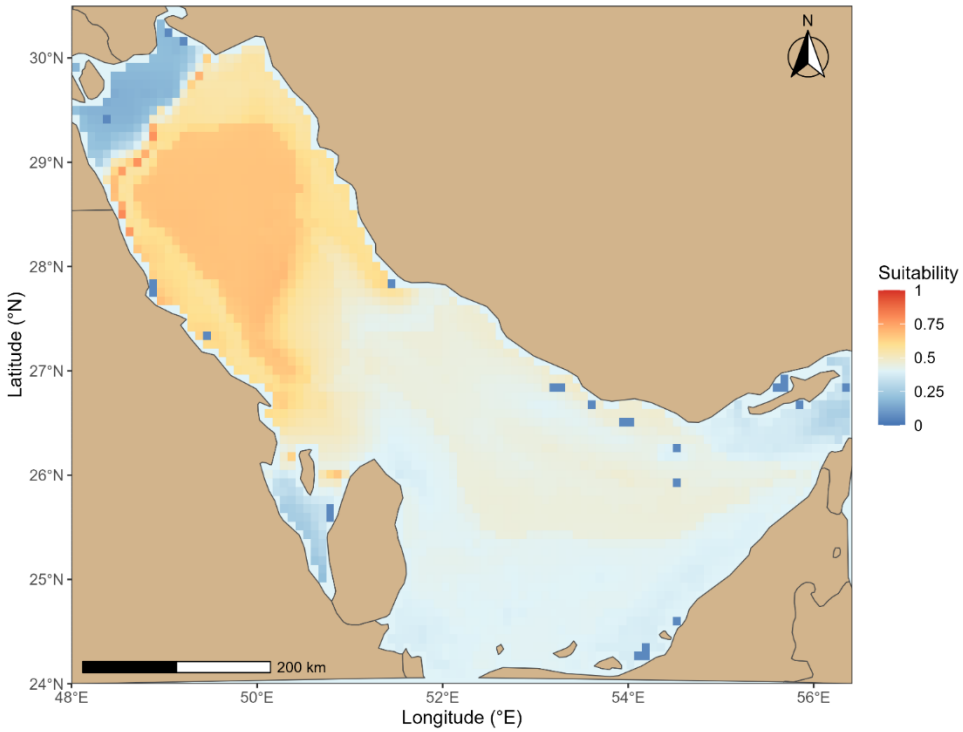


Fig.5. Current habitat suitability for *Caranx ignobilis* in the Persian Gulf predicted by the ensemble model (EMwmean). Colors indicate suitability values ranging from 0 (low) to 1 (high).

Table 3. Geographic coordinates of habitat centroids and centroid shifts under current and future climate scenarios.

Scenario	Longitude (°E)	Latitude (°N)	Longitude change (°E)	Latitude change (°N)	Centroid shift (km)
Current	49.8196	28.2372	0.00	0.00	0.00
SSP2-4.5, 2040	49.4519	29.1434	-0.37	0.91	106.67
SSP5-8.5, 2040	48.8787	29.3155	-0.94	1.08	150.74
SSP2-4.5, 2090	NA	NA	NA	NA	NA
SSP5-8.5, 2090	NA	NA	NA	NA	NA

the largest contiguous area of suitable habitat. At the national level, the coastal waters of Kuwait and Saudi Arabia, along with the northern and central Iranian coasts (provinces of Khuzestan and Bushehr, including Bandar-e Mahshahr, Deylam, Ganaveh, and Bushehr), exhibited the highest habitat suitability. In contrast, the lowest suitability values (HSI < 0.25) were recorded in the southeastern portion of the Gulf, particularly along the coasts of the United Arab Emirates and Oman, near the Strait of Hormuz and the Gulf's outlet. Within Iranian waters, suitability decreased markedly eastward and southward, with the lowest levels observed in Hormozgan Province, around Bandar Abbas and the eastern islands, corresponding to latitudes below 26°N. Under these current climatic conditions, the total area of suitable habitat (HSI ≥ 0.414) within the Gulf was estimated at 48.49 × 10³ km² (Table 4). Under future climate scenarios (SSP2-4.5 and SSP5-8.5 for the 2040s and 2090s), suitable habitat area declined progressively. By the 2040s, the total suitable habitat area had declined substantially to 8.99×10³ km² under SSP2-4.5 and to only 1.26×10³ km² under SSP5-8.5, with remaining habitats largely confined to small patches in the northwestern Gulf. This reduction was more pronounced in the 2090s than in the 2040s, and under the high-emission scenario (SSP5-8.5), habitat loss was greater than under the moderate-emission scenario (SSP2-4.5). By the 2090s, no suitable habitat remained under either SSP2-4.5 or SSP5-8.5, indicating that no cells with HSI above the optimal threshold remained within the study region (reflecting

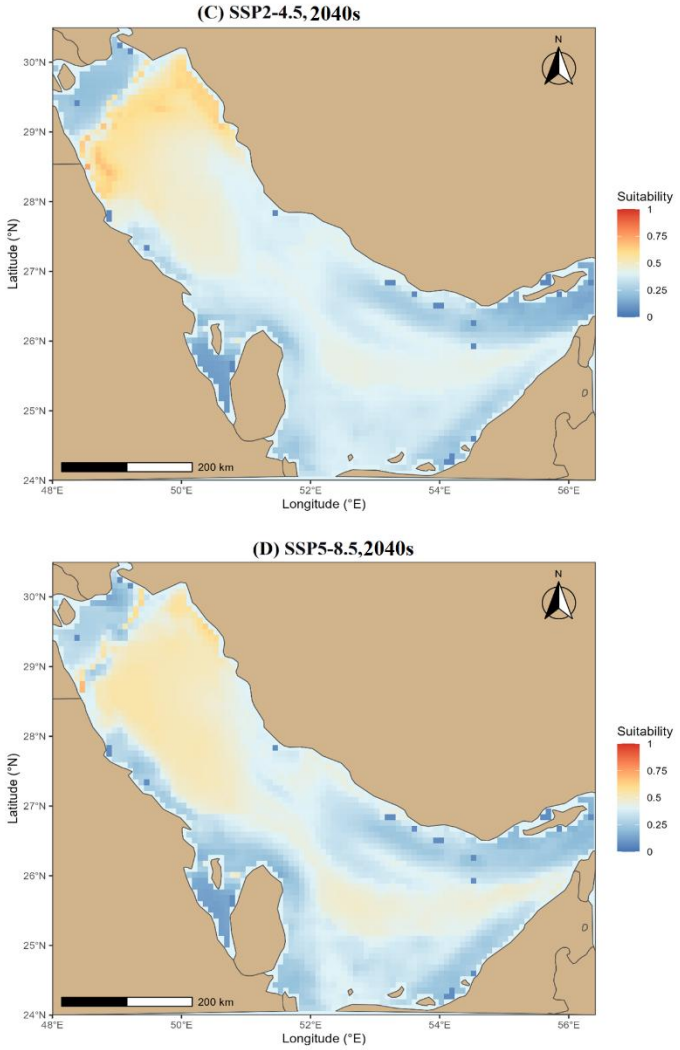


Fig.6. Mid-century habitat suitability for *Caranx ignobilis* in the Persian Gulf predicted by the ensemble model (EMwmean). Colors indicate suitability values ranging from 0 (low) to 1 (high).

Table 4. Projected changes in suitable habitat area, habitat loss, and habitat gain of *C. ignobilis* under current and future climate scenarios (0.414 threshold, 1000km²).

Scenario	Total Habitat Area	Area Lost	Area Gained
Current	48.49	0.00	0.00
SSP2- 4.5, 2040	8.99	45.13	5.63
SSP5- 8.5, 2040	1.26	47.97	0.74
SSP2- 4.5, 2090	0.00	48.49	0.00
SSP5- 8.5, 2090	0.00	48.49	0.00

zero modelled suitable habitat under the applied threshold rather than biological extirpation) (Table 4).

Comparison of the continuous habitat suitability maps (Figs. 6 and 7) showed that under all future climate scenarios for the 2040s, the habitat centroid shifted westward and northward. Based on the habitat centroid for *C. ignobilis* (Table 3), under SSP2-4.5 (2040s) the centroid moved from 49.81°E, 28.23°N to 49.45°E, 29.14°N, and under SSP5-8.5 (2040s) to 48.87°E, 29.31°N, corresponding to longitudinal shifts of -0.37° to -0.94° and latitudinal shifts of +0.91° to +1.08°. For the 2090s, however, no suitable cells were detected under either scenario, resulting in non-calculable centroids (NA). The gained area was considerably smaller than the lost area under all scenarios (Table 4). The habitat centroid shifted by

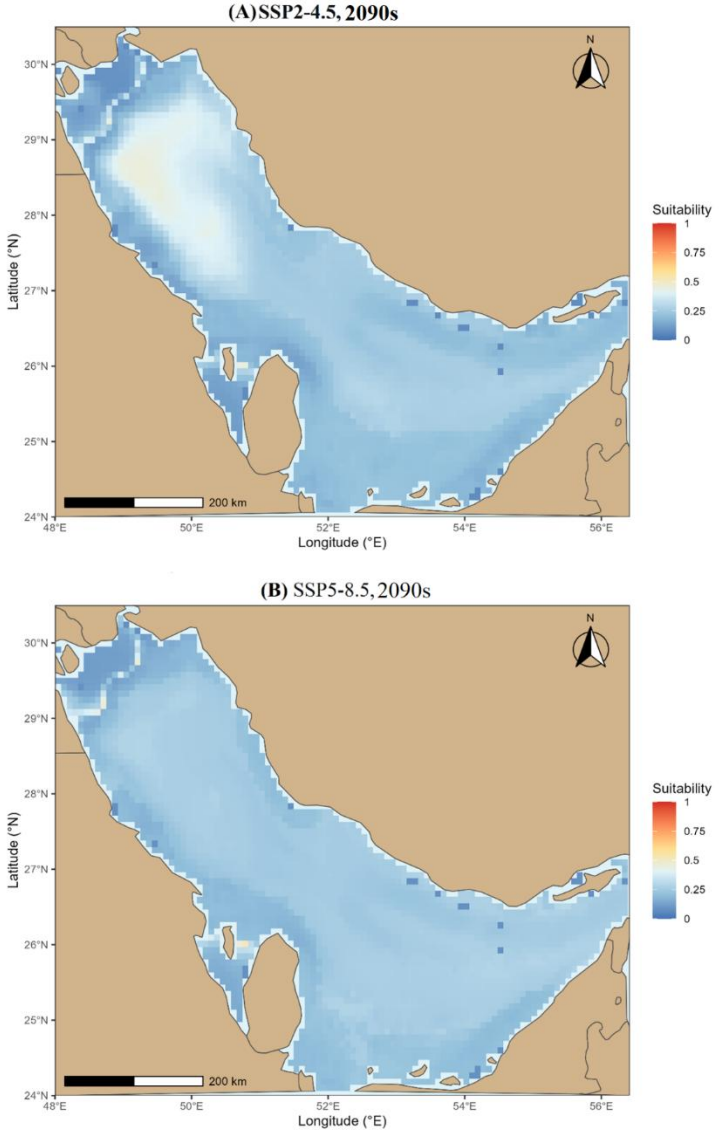


Fig.7. End-of-century (2090s) habitat suitability for *C. ignobilis* in the Persian Gulf predicted by the ensemble model (EMwmean). Colors indicate suitability values ranging from 0 (low) to 1 (high).

106.67 km under SSP2-4.5 in the 2040s and by 150.74 km under SSP5-8.5, indicating a greater displacement under the high-emission scenario.

DISCUSSION

Accuracy evaluation of the model and current distribution of *Caranx ignobilis* habitats: Our results provide new insights into the present habitat distribution of *C. ignobilis* in the Persian Gulf and its potential response to future climate change. By identifying environmentally suitable habitats under current conditions and projecting their future dynamics, this study provides ecological information that can support fisheries management and conservation planning. In particular, identifying habitat hotspots and climatically stable areas may help prioritize monitoring efforts and conservation actions to enhance the long-term resilience of this commercially and ecologically important species.

The current suitable habitat of *C. ignobilis*, as predicted by the weighted-average ensemble model, is distributed throughout much of the Persian Gulf, extending from the northwestern region to the vicinity of the Strait of Hormuz. Areas of highest habitat

suitability are predominantly concentrated in the northwestern and northern offshore waters of the Persian Gulf, particularly adjacent to the coasts of Khuzestan and northern Bushehr provinces (Fig. 5). This spatial pattern suggests that the ensemble model realistically captured the present distribution of suitable habitats for *C. ignobilis* within the Persian Gulf. The ecological realism of the predicted distribution is further supported by independent larval fish surveys conducted in Iranian waters of the Persian Gulf. Studies have consistently reported carangid larvae across all sampled regions since 1995 (Dehghan et al. 1999). The highest larval abundance was recorded in Khuzestan waters (46% relative abundance) during June–July (Dehghan et al. 2002), followed by Bushehr waters, with 6% abundance in Nayband Bay during summer (Rabbaniha 1998; Rabbaniha 2002), 0.07% in central Bushehr estuaries during May–June (Oufi & Bakhtiari 1999; Oufi & Mohammadnejad 2001), and 2.82% around Khark and Kharko Islands during the first half of the year (Rabbaniha 2008). In contrast, larval abundance in Hormozgan waters (Bandar Lengeh) was substantially lower (1.28%; Mortazavi & Seraji 2008). Rabbaniha (2011) further confirmed that the family Carangidae exhibits the highest densities in Khuzestan and Bushehr (Nayband) during the first half of the year, with a clear decline toward the southeast. Although larval distributions cannot be considered direct proxies for adult habitat suitability, the observed northwest-to-southeast decline closely mirrors the spatial suitability gradient predicted by the ensemble model, thereby providing independent support for the model predictions.

Having established the spatial reliability of the ensemble model, we next examined the environmental variables underlying the observed habitat patterns. Climate change substantially alters marine environmental conditions, which consequently influence the distribution and persistence of marine organisms (Harley et al. 2006; Doney et al. 2012). Among the environmental predictors considered in this study, sea surface temperature (SST) emerged as the most influential variable in terms of overall contribution (variable importance), while marginal response curves indicated that primary production and pH also strongly affected habitat suitability. This finding aligns with numerous studies showing that thermal regimes are primary drivers of marine fish distribution and community reorganization under contemporary climate warming (Rutterford et al. 2023; Zhai et al. 2024).

The response curves indicated that habitat suitability peaked at SSTs between 24.98 and 26.29°C, suggesting a relatively narrow thermal optimum for the species. This thermal preference is consistent with the tropical–subtropical distribution of *C. ignobilis* and likely reflects physiological constraints governing habitat selection. Although spawning has been reported to occur at higher temperatures (27.6-29.25°C; Mutia et al. 2015), egg incubation in the closely related carangid *Trachinotus carolinus* is optimal between 24 and 26°C (Weirich et al. 2007; Daly et al. 2019), indicating that this temperature range may represent favorable conditions for early life-history stages across carangids. The Persian Gulf's oceanographic characteristics further reinforce the ecological significance of this thermal optimum. Temperature exhibits pronounced vertical stratification, with surface waters generally ranging from approximately 26.7 to 28°C and cooler temperatures occurring at greater depths (Mubarak & Kubryakov 2001). In the northern Persian Gulf, surface temperatures remain close to 24.8°C, while southern offshore waters commonly range between 26 and 27°C (Mubarak & Kubryakov 2001). These regional temperature conditions closely overlap the thermal optimum predicted by the ensemble model, providing additional ecological support for the observed habitat suitability patterns. Because SST integrates seasonal variability, large-scale climatic oscillations such as El Niño–Southern Oscillation, and long-term ocean warming (L'Heureux et al. 2013; Cai et al. 2021), continued warming is expected to alter water-column structure, dissolved oxygen availability, and habitat quality, thereby driving future shifts in the distribution of *C. ignobilis* (Meyssignac et al. 2017; Roch et al. 2023).

Salinity represented the second most influential environmental predictor in our models. Previous studies have shown that *C. ignobilis* occupies a wide range of salinity conditions, from estuaries and coastal lagoons to offshore coral reefs, with juveniles generally inhabiting low-salinity environments and adults occupying marine habitats (Smith 1991). Our model identified an optimal salinity of 35.21‰, closely matching the lower end of the reported surface salinity range of the surface salinity range reported for the Persian Gulf (36.8-37.5‰) (Reynolds 1993; Mubarak & Kubryakov 2001). This agreement indicates that the predicted salinity preference is ecologically realistic and suggests that small changes in salinity from altered freshwater inputs or evaporation may influence habitat suitability, particularly in shallow coastal environments.

The negative relationship between primary production and habitat suitability is ecologically consistent with the biology and behavior of *C. ignobilis*. This species is primarily associated with coral reef ecosystems, which are typically located in clear, low-nutrient waters with low phytoplankton biomass and high water clarity (Sudekum et al. 1991). As a visual, piscivorous predator that feeds on reef fish and benthic invertebrates (Meyer et al. 2001; Farmer & Wilson 2010), *C. ignobilis* likely benefits from the clear, well-lit waters found in low-productivity environments, which enhance prey detection and foraging efficiency (Lédée et al. 2015). Dietary studies from lagoon systems support this interpretation: stomach content analysis showed that small crustaceans and juvenile fishes made up about 80% of giant trevally diets (Smith 1991; Smith 1992; Mutia 2015), confirming its reliance on small fishes and crustaceans as major prey items. Therefore, the negative relationship between habitat suitability and primary production observed in our model likely reflects habitat characteristics that maximize visual foraging efficiency rather than a direct response to phytoplankton productivity. Studies have also shown that light intensity, time of day, and tidal cycles significantly influence this species' presence and depth use, with individuals moving closer to the surface during low-light periods, presumably to exploit prey aggregations (Lédée et al. 2015). This behavior is consistent with that of other coral reef predators that rely on visual cues for hunting (Lédée et al. 2015).

The impact of future climate scenarios on *C. ignobilis* habitat: Our projections indicate a progressive reorganization of suitable habitat for *C. ignobilis* under future climate scenarios, characterized by contraction in the southeastern Persian Gulf and limited expansion toward the northwestern Gulf during the mid-21st century, followed by the projected zero modelled suitable habitat under the applied threshold by the end of the century (Fig. 7). This does not imply biological extirpation, but rather that no cells exceeded the threshold used for comparative mapping. The projected southeastern contraction and eventual zero modelled suitable habitat for *C. ignobilis* in the Persian Gulf under future climate scenarios are consistent with regional projections for other marine species. Wabnitz et al. (2018) reported that under RCP8.5, the highest species losses in the Gulf are expected along the UAE and Bahrain coasts by 2040s, expanding nearly everywhere by the 2090s, particularly in southern areas. Similarly, Buchanan et al. (2019) identified that most Persian Gulf fish diversity faces high extinction risk under climate change, with coral-associated and commercially targeted species being especially vulnerable. In line with our findings, Ahmadi et al. (2023) projected negative future range changes for *Parastromateus niger* in the Persian Gulf under both RCP4.5 and RCP8.5 scenarios using an ensemble modeling approach, further confirming that habitat contractions are a widespread response among commercially important fish species in the region. Our findings align with these projections, supporting the projection that the southeastern Gulf, which currently supports marginal habitat suitability, will experience the most severe contractions, while the zero modelled suitable habitat by the 2090s reflects a broader regional trend of declining biodiversity under intensifying climate change.

In addition to changes in habitat extent, the projected habitat centroid shifts northwestward, accompanied by a substantially faster contraction of suitable habitat in the southern and southeastern Persian Gulf than expansion toward the northwestern Gulf. This asymmetric response is consistent with the strong spatial heterogeneity of environmental conditions across the Persian Gulf, where hydrographic gradients, freshwater influence in the northern Gulf, and the inflow of oceanic waters through the Strait of Hormuz create distinct thermal and salinity regimes (Reynolds 1993; Mubarak & Kubryakov 2001; Johns et al. 2003). These regional environmental differences are likely to explain the greater persistence of suitable habitats in the northwestern Gulf under future climate scenarios. The projected centroid shift of 150.74 km under SSP5-8.5 is well within *C. ignobilis's* documented movement capacity, which can travel up to 826 km (Chiang et al. 2023). Moreover, this shift represents a population-level distributional change that can be achieved through gradual dispersal, larval settlement, and local extinction–colonization dynamics, rather than requiring individual fish to move the entire distance.

Consistent with these ecological principles, the future response of *C. ignobilis* is likely to be constrained not only by climatic suitability but also by its dependence on coral reef habitats and its site fidelity. Because suitable coral reef habitats are spatially fragmented within the Persian Gulf, successful colonization depends not only on favorable environmental conditions but also on habitat connectivity and availability. Although this species can move long distances (up to 826 km; Chiang et al. 2023), site fidelity and habitat specialization may slow or limit colonization of newly suitable areas at the population level, though not entirely prevent it. Consequently, climate-driven redistribution is expected to occur primarily through habitat loss and spatial displacement rather than extensive range expansion.

Although the ensemble model showed robust predictive performance, several limitations warrant acknowledgment. The accuracy of Species Distribution Models (SDMs) depends strongly on the quality and representativeness of occurrence data. In this study, occurrence records were compiled from the Global Biodiversity Information Facility (GBIF), the Ocean Biodiversity Information System (OBIS), and published geo-referenced field surveys, providing the most comprehensive dataset currently available for *C. ignobilis* across its distribution range. Nevertheless, these datasets remain subject to several sources of uncertainty, including spatial sampling bias, uneven survey effort, temporal inconsistencies, and the over-representation of easily accessible locations. Moreover, reliance on presence-only records requires generating pseudo-absences, introducing additional uncertainty because true absence data are unavailable and model outcomes may be influenced by pseudo-absence selection. As Ray et al. (2024) note, fisheries occurrence records compiled from open-access databases may also reflect catchability and reporting biases. Although integrating multiple independent data sources partially mitigates these limitations, some overestimation or underestimation of habitat suitability in specific regions cannot be ruled out. Future studies should therefore prioritize targeted surveys in under-sampled regions and integrate complementary data sources, such as fisheries-independent surveys, catch statistics, telemetry, and movement data, to improve model robustness and reduce uncertainty in projections of climate-driven habitat change. Incorporating behavioral responses to environmental change may further improve predictive accuracy, as behavioral plasticity can strongly influence species resilience and adaptive capacity under future climate scenarios (Buchholz et al. 2019). Despite these limitations, the present study provides a robust assessment of the current and future habitat suitability of *C. ignobilis* in the Persian Gulf. By identifying areas of habitat persistence, contraction, and potential redistribution under climate change, our findings provide a scientific basis for adaptive fisheries management, conservation planning, and the long-term protection of this commercially and ecologically important reef-associated species (Zhang et al. 2020b; Ray et al. 2024).

Several methodological limitations should be acknowledged. These include the threshold-dependence of the binary habitat classification, the spatial mismatch between global calibration and regional projection, the exclusion of dissolved oxygen due to collinearity with SST, the coarse spatial resolution of environmental layers relative to fine-scale coastal gradients, and the use of pseudo-absences drawn from the global background (see Methods). Each of these is discussed in detail in the corresponding Methods sections.

CONCLUSIONS

This study provides the first comprehensive projection of current and future habitat suitability for *C. ignobilis* in the Persian Gulf using an ensemble species distribution modelling framework based on occurrence records compiled from GBIF, OBIS, and published field surveys together with Bio-ORACLE environmental datasets. Our projections revealed a pronounced northwestward displacement of suitable habitat, accompanied by progressive contraction in the southeastern Persian Gulf, ultimately resulting in zero modelled suitable habitat under the applied threshold by the end of the century under both SSP2-4.5 and SSP5-8.5 scenarios. This does not imply biological extirpation, but rather that no cells exceeded the threshold used for comparative mapping. The projected centroid shift of 150.74 km under SSP5-8.5 is well within the documented movement capacity of *C. ignobilis*, which can travel up to 826 km (Chiang et al. 2023), and represents a population-level distributional change achievable through gradual dispersal and local colonization dynamics. Sea surface temperature, salinity, and primary production were identified as the primary environmental drivers shaping habitat suitability. These findings suggest that climate change is likely to substantially reduce suitable habitat for this ecologically and commercially important reef-associated predator. Consequently, our results provide a scientific basis for adaptive fisheries management, marine spatial planning, and conservation strategies to improve the long-term resilience of *C. ignobilis* populations under future climate change in the Persian Gulf.

REFERENCES

Ahmadi, A.; Imanpour Namin, J.; Sharifian, S. & Daliri, M. 2023. Habitat suitability projections for the Black Pomfret (*Parastromateus niger*) under climate change: an ensemble modeling approach. Iranian Journal of Ichthyology 10(4): 215-224.

Aiello-Lammens, M.E.; Boria, R.A.; Radosavljevic, A.; Vilela, B. & Anderson, R.P. 2015. spThin: an R package for spatial thinning of species occurrence records for use in ecological niche models. Ecography 38(5): 541-545.

Alawad, K.A.; Al-Subhi, A.M.; Alsaafani, M.A. & Alraddadi, T.M. 2023. What causes the Persian Gulf significant summer sea surface temperature warming trend? Atmosphere 14(3): 586.

Allouche, O.; Tsoar, A. & Kadmon, R. 2006. Assessing the accuracy of species distribution models: prevalence, Kappa and the True Skill Statistic (TSS). Journal of Applied Ecology 43(6): 1223-1232.

Araújo, M.B. & New, M. 2007. Ensemble forecasting of species distributions. Trends in Ecology & Evolution 22(1): 42-47.

Assis, J.; Fernández Bejarano, S.J.; Salazar, V.W.; Schepers, L.; Gouvêa, L.; Fragkopoulou, E.; Leclercq, F.; Vanhoorne, B.; Tyberghein, L.; Serrão, E.A.; Verbruggen, H. & De Clerck, O. 2024. Bio-ORACLE v3.0: pushing marine data layers to the CMIP6 earth system models of climate change research. Global Ecology and Biogeography 33: e13897.

Barbet-Massin, M.; Jiguet, F.; Albert, C.H. & Thuiller, W. 2012. Selecting pseudo-absences for species distribution models: how, where and how many?. Methods in Ecology and Evolution 3(2): 327-338.

Bordbar, M.H.; Nasrolahi, A.; Lorenz, M.; Moghaddam, S. & Burchard, H. 2024. The Persian Gulf and Oman Sea: climate variability and trends inferred from satellite observations. Estuarine, Coastal and Shelf Science 296: 108588.

Boyce, D.G.; Tittensor, D.P.; Garilao, C.; Henson, S.; Kaschner, K.; Kesner-Reyes, K.; Pigot, A.; Reyes, R.B.; Reygondeau, G.; Schleit, K.E.; Shackell, N.L.; Sorongon-Yap, P. & Worm, B. 2022. A climate risk index for marine life. Nature Climate Change 12: 854-862.

Brunner, A.; Marquez, J.R.G. & Domisch, S. 2024. Downscaling future land cover scenarios for freshwater fish distribution models under climate change. Limnologica 104: 126139.

Buchanan, J.R.; Ralph, G.M.; Krupp, F.; Harwell, H.; Abdallah, M.; Abdulqader, E.; Al-Husaini, M.; Bishop, J.M.; Burt, J.A.; Choat, J.H. & Collette, B.B. 2019. Regional extinction risks for marine bony fishes occurring in the Persian Gulf. Biological Conservation 230: 10-19.

Buchholz, R.; Banusiewicz, J.D.; Burgess, S.; Crocker-Buta, S.; Eveland, L. & Fuller, L. 2019. Behavioural research priorities for the study of animal response to climate change. Animal Behaviour 150: 127-137.

Cai, W.; Santoso, A.; Collins, M.; Dewitte, B.; Karamperidou, C.; Kug, J.-S.; Lengaigne, M.; McPhaden, M.J.; Stuecker, M.F. & Taschetto, A.S. 2021. Changing El Niño–Southern oscillation in a warming climate. Nature Reviews Earth & Environment 2(9): 628-644.

Chamberlain, S.A. & Boettiger, C. 2017. R, Python, and Ruby clients for GBIF species occurrence data. PeerJ Preprints e3304v1.

Chen, Y.; Shan, X.; Gorfine, H.; Dai, F.; Wu, Q.; Yang, T.; Shi, Y. & Jin, X. 2023. Ensemble projections of fish distribution in response to climate changes in the yellow and Bohai seas. China. Ecological Indicators 146: 109759.

Chen, Y.; Shan, X.; Ovando, D.; Yang, T.; Dai, F. & Jin, X. 2021. Predicting current and future global distribution of black rockfish (*Sebastes schlegelii*) under changing climate. Ecological Indicators 128: 107799.

Cheung, W.W.L.; Brodeur, R.D.; Okey, T.A. & Pauly, D. 2015. Projecting future changes in distributions of pelagic fish species of Northeast Pacific shelf seas. Progress in Oceanography 130: 19-31.

Chiang, W.C.; Lin, S.J.; Soong, K.Y.; Liao, T.Y.; Chen, Y.Y.; Ho, Y.S. & Musyl, M.K. 2023. Movement patterns and habitat use of adult giant trevally (*Caranx ignobilis*) in the South China Sea. Marine Biology 170: 65.

Copernicus Climate Change Service (C3S). 2024. Global climate highlights 2024. https://climate.copernicus.eu/global-climate-highlights-2024

Daly, R.; Filmalter, J.D.; Daly, C.A.K.; Bennett, R.H.M.; Pereira, A.M.; Mann, B.Q.; Dunlop, S.W. & Cowley, P.D. 2019. Acoustic telemetry reveals multi-seasonal spatiotemporal dynamics of a giant trevally Caranx ignobilis aggregation. Marine Ecology Progress Series 621: 185-197.

Dehghan Madiseh, S. 1998. Identification and density determination of ichthyoplankton in Khuzestan creeks. Khuzestan Fisheries Research Center, Ahvaz.

Dehghan Madiseh, S. 1999. Diversity and abundance of ichthyoplankton (fish larval stages) in the western coasts of Khuzestan. Khuzestan Fisheries Research Center, Ahvaz.

Dehghan Madiseh, S. 2002. Diversity and abundance of ichthyoplankton (fish larval stages) in Khuzestan province waters - Phase 3: Eastern coasts. Khuzestan Fisheries Research Center, Ahvaz.

Eagderi, S.; Mouludi-Saleh, A.; Fricke, R.; Alavi-Yeganeh, M.S.; Mousavi-Sabet, H. & Cicek, E. 2026. Fishes of the Sea of Oman. Iranian Journal of Ichthyology 13(Special Issue): 1-152.

FAO. 2018. The state of world fisheries and aquaculture 2018 – meeting the sustainable development goals. Rome. http://www.fao.org/3/I9540EN/i9540en.pdf

Froese, R.; Pauly, D. 2024. FishBase: world wide web electronic publication. www.fishbase.org, version (02/2024). (web resource). fishbase.se

Gregorich, M.; Strohmaier, S.; Dunkler, D. & Heinze, G. 2021. Regression with highly correlated predictors: variable omission is not the solution. International Journal of Environmental Research and Public Health 18(8): 4259.

Han, H.B.; Yang, C.; Jiang, B.H.; Shang, C.; Sun, Y.Y.; Zhao, X.Y.; Xiang, D.L.; Zhang, H. & Shi, Y.C. 2023. Construction of chub mackerel (*Scomber japonicus*) fishing ground prediction model in the northwestern Pacific Ocean based on deep learning and marine environmental variables. Marine Pollution Bulletin 193: 115158.

Johns, W.; Yao, F.; Olson, D.; Josey, S.; Grist, J. & Smeed, D. 2003. Observations of seasonal exchange through the Straits of Hormuz and the inferred heat and freshwater budgets of the Persian Gulf. Journal of Geophysical Research: Oceans 108(C12): 1-18.

Kaky, E.; Nolan, V.; Alatawi, A. & Gilbert, F. 2020. A comparison between ensemble and MAXNET species distribution modelling approaches for conservation: a case study with Egyptian medicinal plants. Ecological Informatics 60: 101150.

Lachkar, Z.; Pauluis, O.; Paparella, F.; Khan, B. & Burt, J.A. 2025. Local and remote climatic drivers of extreme summer sea surface temperatures in the Persian Gulf. Ocean Science 21(6): 3241-3263.

Lédée, E.J.I.; Heupel, M.R.; Tobin, A.J. & Simpfendorfer, C.A. 2015. Movements and space use of giant trevally in coral reef habitats and the importance of environmental drivers. Animal Biotelemetry 3(1): 6.

Lee, D.; Son, S.; Kim, W.; Park, J.; Joo, H. & Lee, S. 2018.

Spatio-temporal variability of the habitat suitability index for chub mackerel (*Scomber japonicus*) in the East/Japan Sea and the South Sea of South Korea. Remote Sensing 10(6): 938.

L'Heureux, M.L.; Collins, D.C. & Hu, Z.-Z. 2013. Linear trends in sea surface temperature of the tropical Pacific Ocean and implications for the El Niño-Southern Oscillation. Climate Dynamics 40(5): 1223-1236.

Li, G.; Cao, J.; Zou, X.; Chen, X. & Runnebaum, J. 2016. Modeling habitat suitability index for Chilean jack mackerel (*Trachurus murphyi*) in the South East Pacific. Fisheries Research 178: 47-60.

Lobo, J.M.; Jiménez-Valverde, A. & Real, R. 2007. AUC: a misleading measure of the performance of predictive distribution models. Global Ecology and Biogeography 17(2): 145-151.

Meyer, C.G.; Holland, K.N. & Papastamatiou, Y.P. 2007. Seasonal and diel movements of giant trevally *Caranx ignobilis* at remote Hawaiian atolls: implications for the design of marine protected areas. Marine Ecology Progress Series 333: 13-25.

Meyssignac, B.; Piecuch, C.; Merchant, C.; Racault, M.-F.; Palanisamy, H.; MacIntosh, C.; Sathyendranath, S. & Brewin, R. 2017. Causes of the regional variability in observed sea level, sea surface temperature and ocean colour over the period 1993–2011. In *Integrative Study of the Mean Sea Level and Its Components*. Cham, Switzerland: Springer. pp. 191-219.

Mortazavi, M. & Seraji, F. 2008. Ecological study of artificial habitats in Hormozgan province waters (Bandar Lengeh). Iranian Fisheries Research Institute, Tehran.

Mubarak, W.A.-M. & Kubryakov, A. 2001. Hydrological structure of waters of the Persian Gulf according to the data of observations in 2001. Physical Oceanography 11(5): 459-471.

Mutia, T.M. 2015. Induced breeding of malipulo *Caranx ignobilis*. NFRDI Fisheries Biological Research Centre, Butong, Taal, Batangas. https://repository.seafdec.org.ph/handle/10862/2792.

Nisin, K.M.N.; M., K.R.S. & Paul Sreeram, M. 2023. Change in habitat suitability of the invasive snowflake coral (*Carijoa riisei*) during climate change: an ensemble modelling approach. Ecological Informatics Eco. Inform. 76: 102145.

NOAA National Centers for Environmental Information (NCEI). 2024. Assessing the global climate in 2024. https://www. ncei.noaa.gov/news/global-climate-202413

Oufi, F. & Bakhtiari, M. 1999. Abundance and diversity of ichthyoplankton (fish larval stages) in Bushehr province waters (Bushehr creeks). Persian Gulf Fisheries Research Center, Bushehr.

Oufi, F. & Mohammadnejad, J. 2001. Abundance and diversity of ichthyoplankton (fish larval stages) in Bushehr province waters (Ziarat creek - Nayband). Persian Gulf Fisheries Research Center, Bushehr.

Papastamatiou, Y.P.; Meyer, C.G.; Kosaki, R.K.; Wallsgrove, N.J. & Popp, B.N. 2015. Movements and foraging of predators associated with mesophotic coral reefs and their potential for linking ecological habitats. Marine Ecology Progress Series 521: 155-170.

Pitman, K.J.; Moore, J.W.; Huss, M.; Sloat, M.R.; Whited, D.C.; Beechie, T.J.; Brenner, R.; Hood, E.W.; Milner, A.M.; Pess, G.R.; Reeves, G.H. & Schindler, D.E. 2021. Glacier retreat creating new Pacific salmon habitat in western North America. Nature Communication 12(1): 6816.

Poorbagher, H., & Eagderi, S. (2024). Predicting the distribution of fish community in the Persian Gulf using joint species distribution modelling with a latent variable model. Iranian Journal of Ichthyology 11(1): 69-78.

Provoost, P. & Bosch, S. 2022. robis: R client for the OBIS API. GitHub. https://github.com/iobis/robis.

Rabbaniha, M. 1998. Diversity and abundance of ichthyoplankton (fish larval stages) in Nayband Bay. Persian Gulf Fisheries Research Center, Bushehr.

Rabbaniha, M. 2002. Abundance and diversity of fish larvae in the northern coasts of Bushehr province (Frakeh estuary to Bandar Genaveh). [Master's thesis]. Tarbiat Modares University, Faculty of Marine Sciences and Natural Resources.

Rabbaniha, M. 2008. Identification of diversity and distribution pattern of fish larvae in the coral island ecosystem of Kharg and Kharko in the Persian Gulf using Geographic Information System (GIS). [Doctoral dissertation]. Islamic Azad University, Science and Research Branch.

Ray, A.; Mondal, S.; Lee, M.-A.; Lu, Q.-H.; Sihombing, R.I. & Wang, Y.-C. 2024. Impact of climate change on the waters off southwest Taiwan: predicted alterations in moonfish distribution and catch rates. Frontiers in Marine Science 11: 1444252.

Reynolds, R.M. 1993. Physical oceanography of the Gulf, Strait of Hormuz, and the Gulf of Oman—results from the Mt Mitchell expedition. Marine Pollution Bulletin 27: 35-59.

Roch, M.; Brandt, P. & Schmidtko, S. 2023. Recent large-scale mixed layer and vertical stratification maxima

changes. Frontiers in Marine Science 10: 1277316.

Rutterford, L.A.; Simpson, S.D.; Bogstad, B.; Devine, J.A. & Genner, M.J. 2023. Sea temperature is the primary driver of recent and predicted fish community structure across Northeast Atlantic shelf seas. Global Change Biology 29(9): 2510-2521.

Schickele, A.; Goberville, E.; Leroy, B.; Beaugrand, G.; Hattab, T.; Francour, P. & Raybaud, V. 2020a. European small pelagic fish distribution under global change scenarios. Fish and Fisheries 22(1): 212-225.

Schickele, A.; Leroy, B.; Beaugrand, G.; Goberville, E.; Hattab, T.; Francour, P. & Raybaud, V. 2020b. Modelling European small pelagic fish distribution: methodological insights. Ecological Modelling 416: 108902.

Shi, Y.; Kang, B.; Fan, W.; Xu, L.; Zhang, S.; Cui, X. & Dai, Y. 2023a. Spatio-temporal variations in the potential habitat distribution of Pacific sardine (*Sardinops sagax*) in the Northwest Pacific Ocean. Fishes 8(2): 86.

Smith, G.C. 1991. Abundance, diet and growth of Caranx ignobilis and Caranx melampygus (Carangidae) in the Hanalei River Estuary, North Kauai, Hawaii. [M.ScM.Sc. thesis]. University of Hawaii.

Smith, G.C. 1992. Occurrence and diets of juvenile *Caranx ignobilis* and *Caranx melampygus* (Teleostei: Carangidae) in the Hanalei River Estuary, North Kauai, Hawaii. Pacific Science 46(1): 103.

Sudekum, A.E.; Parrish, J.D.; Radtke, R.L. & Ralston, S. 1991. Life history and ecology of large jacks in undisturbed, shallow, oceanic communities. Fishery Bulletin 89: 493-513.

Thuiller, W.; Georges, D.; Gueguen, M.; Engler, R.; Breiner, F.; Lafourcade, B.; Patin, R. & Blancheteau, H. 2025. biomod2: ensemble platform for species distribution modeling. R package version 4.2-6-2. https://CRAN.R-project.org/package=biomod2.

Thuiller, W.; Guéguen, M.; Renaud, J.; Karger, D.N. & Zimmermann, N.E. 2019. Uncertainty in ensembles of global biodiversity scenarios. Nature Communications 10(1): 1446.

Thuiller, W.; Lafourcade, B.; Engler, R. & Araújo, M.B. 2009. BIOMOD – a platform for ensemble forecasting of species distributions. Ecography 32(3): 369-373.

Torrejón-Magallanes, J.; Angeles-González, L.E.; Csirke, J.; Bouchon, M.; Morales-Bojórquez, E. & Arreguín-Sánchez, F. 2021. Modeling the Pacific chub mackerel (*Scomber japonicus*) ecological niche and future scenarios in the northern Peruvian current system. Progress in Oceanography 197: 102672.

Tyberghein, L.; Verbruggen, H.; Pauly, K.; Troupin, C.; Mineur, F. & De Clerck, O. 2011. Bio-ORACLE: a global environmental dataset for marine species distribution modelling. Global Ecology and Biogeography 21(2): 272-281.

Wabnitz, C.C.; Lam, V.W.; Reygondeau, G.; Teh, L.C.; Al-Abdulrazzak, D.; Khalfallah, M.; Pauly, D.; Palomares, M.L.D.; Zeller, D. & Cheung, W.W. 2018. Climate change impacts on marine biodiversity, fisheries and society in the Persian Gulf. PLoS One 13(5): e0194537.

Wei, T. & Simko, V. 2021. R package 'corrplot': visualization of a correlation matrix (version 0.92). https://github.com/taiyun/corrplot.

Weirich, C.R. & Riley, K.L. 2007. Volitional spawning of Florida pompano, *Trachinotus carolinus*, via administration of gonadotropin releasing hormone analogue (GnRHa). Journal of Applied Aquaculture 19(3): 47-60.

World Meteorological Organization (WMO). 2024. State of the Global Climate 2024. Geneva. WMO-No. 1368. https://public.wmo.int/sites/default/files/2025-03/WMO-1368-2024_en.pdf

Xu, Y.; Ma, L.; Sui, J.X.; Li, X.Z.; Wang, H.F. & Zhang, B.L. 2024. Projections of climate-driven biogeographical changes of benthic mollusks in the Yellow Sea and East China Sea. Marine Environmental Research 197: 11.

Yang, T.; Liu, X. & Han, Z. 2022. Predicting the effects of climate change on the suitable habitat of Japanese Spanish mackerel (*Scomberomorus niphonius*) based on the species distribution model. Frontiers in Marine Science 9: 927790.

Zhai, P.; Liu, S. & Chen, Y. 2024. Global chlorophyll trends and implications for fish habitat suitability under climate change. Remote Sensing 16: 2033.

Zhang, C.I.; Lee, J.B.; Kim, S. & Oh, J.-H. 2000. Climatic regime shifts and their impacts on marine ecosystem and fisheries resources in Korean waters. Progress in Oceanography 47(2-4): 171-190

Zhang, Z.; Mammola, S. & Zhang, H. 2020b. Does weighting presence records improve the performance of species distribution models? A test using fish larval stages in the Yangtze Estuary. Science of the Total Environment 741: 140393.

Iran. J. Ichthyol. (2026) 13(3): 168-186
P-ISSN: 2383-1561; E-ISSN: 2383-0964
http://www.ijichthyol.org
© 2026 Iranian Society of Ichthyology
doi: 10.22034/iji.v13i3.1152

مقاله کامل

پیش‌بینی تغییرات مطلوبیت زیستگاه ماهی گیش بزرگ *Caranx ignobilis* (Forsskål, 1775) در خلیج فارس با استفاده از مدل‌های تجمیعی توزیع گونه‌ها

حامد موسوی‌ثابت*، ابوذر حبیبی

گروه شیلات، دانشکده منابع طبیعی، دانشگاه گیلان، صومعه‌سرا، ایران.

چکیده: درک تأثیرات تغییر اقلیم بر زیستگاه‌های دریایی برای پیش‌بینی تغییرات آینده در پراکنش گونه‌ها و پشتیبانی از مدیریت پایدار شیلات ضروری است؛ به‌ویژه برای شکارچیان رأس هرم غذایی که از اهمیت تجاری برخوردارند. در این مطالعه، مطلوبیت زیستگاه کنونی و آینده گونه *Caranx ignobilis*(Forsskål, 1775) در خلیج فارس با استفاده از مختصات حضور استخراج‌شده از پایگاه‌های داده جهانی GBIF و OBIS، گزارش‌های منتشرشده از بررسی‌های میدانی و پیش‌بین‌های محیطی Bio-ORACLE مدل‌سازی شد. شش الگوریتم منفرد و سه روش تجمیعی با استفاده از بسته biomod2 اجرا شدند. مدل تجمیعی EMwmean با مقادیر AUC برابر با ۰,۹۹۲ و TSS برابر با ۰,۹۲۳ برای پیش‌بینی‌های نهایی انتخاب شد؛ زیرا با ادغام چند الگوریتم، سوگیری وابسته به هر مدل را کاهش می‌دهد. براساس تحلیل اهمیت متغیرها، دمای سطح دریا (SST)، شوری و تولید اولیه مهم‌ترین پیش‌بین‌های محیطی مؤثر بر مطلوبیت زیستگاه بودند. پیش‌بینی‌ها تحت سناریوهای SSP2-4.5 و SSP5-8.5 از انقباض تدریجی زیستگاه مناسب در بخش جنوب‌شرقی خلیج فارس و جابجایی شمال‌غربی مرکز ثقل زیستگاه حکایت داشتند. به‌طور مشخص، مساحت زیستگاه مناسبِ مدل‌سازی‌شده، که در شرایط کنونی $۴۸,۴۹\times۱۰^{۳}$ کیلومتر مربع برآورد شد، پیش‌بینی می‌شود تا دهه ۲۰۹۰ در هر دو سناریو به نزدیک صفر برسد. این نتیجه نشان‌دهنده صفرشدن مساحت زیستگاه مناسبِ مدل‌سازی‌شده بر اساس آستانه به‌کاررفته است و به‌معنای انقراض زیستی گونه نیست. یافته‌های این مطالعه اطلاعاتی مکانی و صریح برای پشتیبانی از مدیریت سازگارانه شیلات و برنامه‌ریزی حفاظتی فراهم می‌کنند و می‌توانند به تقویت تاب‌آوری بلندمدت این شکارچی وابسته به صخره‌های مرجانی، با اهمیت بوم‌شناختی و تجاری، در برابر تغییر اقلیم در خلیج فارس کمک کنند.

کلمات‌کلیدی: تغییر اقلیم، مدل‌سازی تجمیعی، خلیج فارس، مطلوبیت زیستگاه، *Caranx ignobilis*، مدل‌سازی توزیع گونه‌ها